19th International Conference on Renewable Energies and Power Quality (ICREPQ'21)
Almeria (Spain), 28th to 30th July 2021
Renewable Energy and Power Quality Journal (RE&PQJ)
ISSN 2172-038 X, Volume No.19, September 2021

Dual-Axis Tracking Electrical Drives for Solar Power Tower

W. M. Hamanah[1], A. Salem[1], and M. A. Abido[1,2], T. G. Habetler[3], and A. M. Qwbaiba[3]

1. Department of Electrical Engineering, King Fahd University for Petroleum and Minerals, Dhahran, 31261, KSA
2. K.A.CARE Energy Research & Innovation Center (ERIC), King Fahd University for Petroleum and Minerals, KSA

[3]School of Electrical and Computer Engineering, Georgia Institute of Technology, Atlanta, GA, 30332, USA
Fax number: +966-3-8603535,

e-mail: g201105910@kfupm.edu.sa, asalem@kfupm.edu.sa, mabido@kfupm.edu.sa, tom.habetler@ece.gatech.edu, qwbaiban@gatech.edu

Abstract. The solar power tower (SPT) is an effective thermal renewable energy source aiming to absorb direct sunbeams on a central collector using thousands of electrical drive-based moved reflectors. The reflector tracking system's accuracy depends on the utilized drive system effectiveness and the used control technique robustness. In this paper, the different electric drives system used in SPT trackers, including motors and power electronic converters, are presented and discussed. Besides, this paper highlighted the advantages and drawbacks of each drive system. Additionally, a dual-axis tracking technique employing the azimuth-elevation tracking approach is discussed and derived for a dual linear actuator heliostat. Moreover, an SPT heliostat prototype using a DC drive system, designed and implemented locally, is discussed and analyzed. The experimental results show the effectiveness of the proposed platform.

Keywords: Concentrated Solar Power; Heliostat Control System; Electric Drives; Power Electronic Converters.

1. Introduction

Renewable energy sources are the most cost-effective, dependable, and safe solution for expanding access to advanced energy resources. Thermal-based solar energy, called concentrated solar power (CSP), is an exciting green energy technology that depends on gathering sunbeams on a receiver by using a movable collector. Then, the collected thermal energy may be used for thermal feed systems such as chillers, or other uses, such as electricity generation and water desalination [1]. The Solar Power Tower (SPT) technology is the most effective among the various CSP technologies, where if the commercial production costs are minimized, SPT topology can be flourish. As a result, long-term electricity costs are less than other topologies [2], [3]. The SPT principle uses a mirror called heliostats, reflecting sunbeams at a particular point on a collector, called *target*. A heliostat is usually a flat mirror assisted by a rotating mechanical structure that controls the sunbeams by a dual-axis tracking device.

Recently, heliostat's work focuses on monitoring and precision tracking devices and systems tuning. SPT heliostat fields typically face the challenges of cost-effectiveness and poor energy efficiency due to the high number of sensors used. A cluster management strategy is used to reduce the number of sensors used, reduce field costs, and achieve fair precision [4]. Extensive analysis of existing larger-scale SPT systems has been introduced in [5], [6] with a view to the tracking of error causes and critical calibration systems specifications. Moreover, strategies were proposed for enhancing energy efficiency.

In general, an SPT plant's performance depends on the heliostats' capacity to reflect the sunbeam to the target point. [7]. Along the year, reflection needs an active drive mechanism to pass the heliostat across a broad range of azimuth and elevation angles to represent the sunbeams accurately. A costly power-modulator, control system, gearbox, and motor are required for the exact and reliable driving system. Moreover, several thousands of heliostat units are needed in one SPT field, making the drive system contribute 30-40% of the overall SPT cost [8], [9]. Therefore, it is essential to provide an advanced and economic heliostat drive device.

The latest works show part-level differences in SPT-related heliostat drive systems concerning electrical motors and power-electronic converters, as far as the authors are aware. Thus, this paper offers a study of the SPT technology supremacy about device performance. The various heliostat drive systems are reviewed. The drive system, including the electric motors and their power-electronic converters, are described and discussed. Comparing the different drive systems in terms of their cost and performance is presented. The azimuth-elevation approach controls a two linear actuators heliostat based on the dual-axis tracking technique.

The remainder of this paper is structured as follows. Firstly, the SPT's superiority over the different CSP technologies is highlighted. In Section 3, the dual-axis tracing based on the azimuth-elevation approach is derived and discussed for a two linear actuator heliostat. In Section 4, the different drive systems used in heliostat SPT systems are discussed and analyzed. The advantages, the drawbacks, and the application for each drive system are emphasized. A prototype for the dual-axis tracker based on a DC drive system, implemented in KSA, is discussed and analyzed in Section 5. Finally, the paper's conclusion is derived.

2. Solar Power Tower System

Scientists divide the sunbeams coming to the ground into three distinct groups. Some radiations are direct, reflected, and diffuse. According to the sunbeam concentration process, CSP technologies can be divided into point and line concentrations. Two well-known topologies are based on the online concentration: Parabolic Trough Collector (PTC) and Linear Fresnel Reflector (LFC). Conversely, two different topologies are based on point concentration: Solar-Power Tower (SPT) and Parabolic Dish Collector (PDC), as shown in Figure 1, [10] and [11].

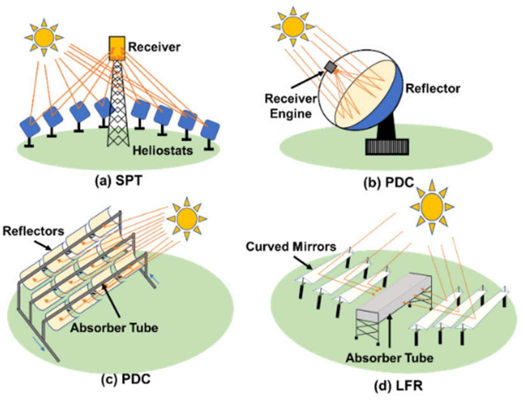

Figure 1. Different CSP topologies

As shown in Figure 1(a), SPT is also known as central receiver systems. A heliostat field collector reflects and concentrates the sunbeams onto a prominent collector placed on a tower. A heliostat unit is a flat mirror or multi flat mirrors supported by a mechanical structure that follows the sun movement using a dual-axis tracking system. The SPT system produces relatively high temperatures, i.e., 540 – 840^{o} C, capable of generating high-pressure steam to move the turbines. Therefore, the cost of thermal storage is reduced substantially [12]. The SPT can be joined with steam cycles with a thermal system efficiency of 40% and can be increased, by the combined cycle, to reach 55% [7]. It could be observed that overall, the share of SPT projects has increased during the last decade compared to other CSP projects in 15 countries, with 53 plants generating around 3442 MW [13].

The overall comparison for the different topologies can be summarized as that the SPT has higher overall efficiency and higher temperature levels [14]. However, an SPT power plant's effectiveness depends on the heliostats' ability to reflect the receiver's sunbeams. Reflecting the sunbeams for a whole year requires a drive system to move the heliostat over a wide range of azimuth and elevation angles, representing a challenge in developing novel, efficient and low-cost drive systems. Heliostats are considered the bulk cost of SPT plants as they contribute about 40% of the power plants' overall cost [15]-[17]. The following sections describe different drive systems with their motors and the power electronic converters due to the drive system's high share of heliostat unit cost. Besides, various drive system mechanisms, operation, and control techniques are discussed along with their pros and cons.

3. Dual-Axis Tracking Approach

The solar tracking systems must be adjusted continuously and accurately to collect the traveling sunbeams' energy. Two well-known tracking techniques are used in CSP systems: single-axis and dual-axis tracking techniques. The single-axis tracking system is less costly and is easily controlled. However, its efficiency is lower compared with the dual-axis solar tracking approach. Three sets of angles must be defined to achieve accurate tracking. These are the sun, tower, and heliostat angles.

A. Sun Angles

Firstly, elevation angle (α_s) and solar azimuth angle (γ_s) (See Figure 2-a) are needed to define the sun position. The elevation angle is expressed by [18]:

$$\alpha_s = 90 - \cos^{-1}[\cos(\varphi)\cos(\delta)\cos(\omega) + \sin(\varphi)\sin(\delta)] \; ; \delta = 23.45 \sin\left(360 \times \frac{284+n}{365}\right) \quad (1)$$

The angle δ is the declination angle, φ is the latitude angle, ω is the time angle, and n is the day number; n = 1 on Jan. 1st every year. The zenith angle ($\theta_z = 90 - \alpha_s$) is the angle of incidence of beam radiation on a horizontal surface. The angle γ_s can be calculated as:

$$\gamma_s = sign(\omega)\left|cos^{-1}\left(\frac{\cos(\theta_z)\sin(\varphi)-\sin(\delta)}{\sin(\theta_z)\cos(\varphi)}\right)\right| + 180; \; \theta_z \neq 0 \quad (2)$$

Depending on time and date values (year, month, day, hour, minute, and second) and location (longitude (φ) and latitude angles), the solar elevation and azimuth angles are described in Figure 2-a.

B. Tower and heliostat model

Like the heliostat positioning angles, two angles are needed to identify the tower position: elevation and azimuth angles. The tower elevation angle (α_T) is a function of the tower height (*H*), the heliostat height (*h*), and the distance of the heliostat from the tower (*R*) (See Figure 2-b). In addition to the elevation angle, the target position of the tower is defined by the azimuth target angle (γ_T) which is referenced by the North direction of the heliostat and tower. The sunbeam tracking is identified by two angles, called heliostat angles, as described in Figure 2-c. These angles are heliostat elevation angle (α^*_H) and heliostat azimuth angle (γ^*_H). The following approach can be used to calculate the heliostat tracking angles. Firstly, the sun and tower angles are converted to Cartesian coordinates as described by (3), (4). The normal mirror vector based on three-dimensional Cartesian form (x, y, and z) can be calculated using (5). Finally, the heliostat tracking angles α^*_H and γ^*_H can be calculated using (6).

$$\begin{aligned} z_1 &= \sin(\alpha_s) \\ x_1 &= \cos(\alpha_s) * \cos(-\gamma_s) \\ y_1 &= \cos(\alpha_s) * sin(-\gamma_s) \end{aligned} \quad (3)$$

$$\begin{aligned} z_2 &= \sin(\alpha_T) \\ x_2 &= \cos(\alpha_T) * \cos(-\gamma_T) \\ y_2 &= \cos(\alpha_T) * sin(-\gamma_T) \end{aligned} \quad (4)$$

$$\begin{aligned} x &= \frac{x_1 - x_2}{2} + x_2 \\ y &= \frac{y_1 - y_2}{2} + y_2 \\ z &= \frac{z_1 - z_2}{2} + z_2 \end{aligned} \quad (5)$$

$$\alpha^*_H = sin^{-1}\left(\frac{z}{\sqrt{x^2+y^2+z^2}}\right)$$

$$\gamma^*_H = \left|\begin{array}{ll} tan^{-1}(-y/x) & if\ x > 0 \\ tan^{-1}(-y/x) + 90 & if\ x < 0, and\ \ y \geq 0 \\ tan^{-1}(-y/x) - 90 & if\ x < 0, and\ \ y < 0 \\ 90 & if\ x = 0, and\ \ y > 0 \\ -90 & if\ x = 0, and\ \ y < 0 \\ \text{undefined} & if\ x = 0, and\ \ y = 0 \end{array}\right| \quad (6)$$

4. Electrical Drives for Dual-Axis Tracking Systems

According to the mathematical model described in the abovementioned section, an accurate electrical drive system is needed to track the sunbeams continuously. A generic block diagram for an electrical drive system is shown in Figure 3. The system is composed of a power electronic converter that modulates the supply according to the used motor. The sensors are used to transfer the measured signals to the digital controller to achieve the control command accurately. The control technique is implemented within the digital controller to steer the power electronic converter with a suitable train of pulses ideal for the control command [19]. For a heliostat dual-axis solar tracking system, the mechanical load represents the mirror, the movable structure, and the gearbox coupled with the motor shaft to transfer the mechanical energy to a suitable form; for instance, from rotational motion to translational motion for linear actuators. The sensor needed for such a system is a position sensor used to feedback the mirror position measurement. Based on the electrical source nature, AC or DC, and the motor type, the power electronic converter can be selected. On the other hand, motor selection depends on the connected load's mechanical characteristics. The following subsections illustrate the most well-known electrical drive systems used for SPT dual-axis trackers.

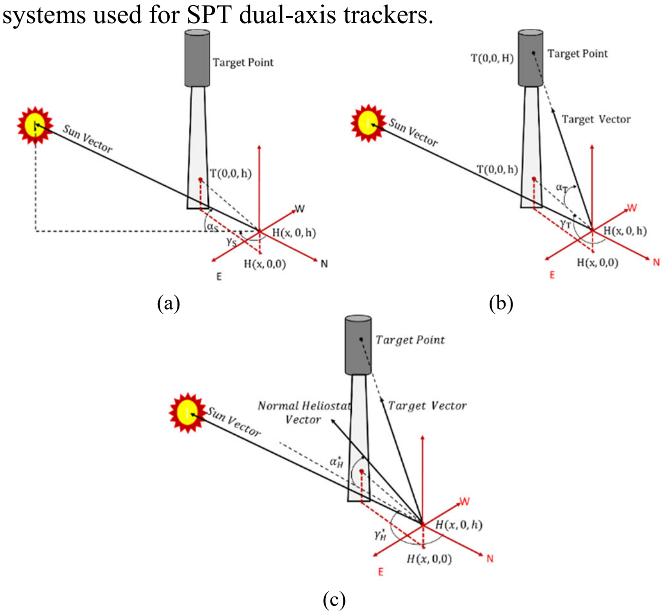

Figure 2. The dimensions for (a) sun elevation and azimuth angles, (b) tower elevation and azimuth angles, and (c) heliostat elevation and azimuth angles.

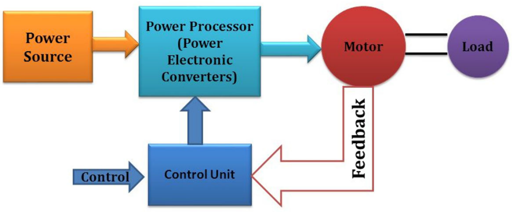

Figure 3. General block diagram describing the electrical drive system components

A. DC Drive

DC motors have the advantages of fast starting, acceleration, deceleration, forward, and reverse responses. Besides, DC motors are preferred due to their simple control for a wide range of speed. Different DC motors can be used in SPT applications, i.e., shunt, compound, and permanent magnet DC motors [20]. Firstly, DC drives have been utilized for an old SPT heliostat design, as described in [21], [22].

A switched-mode DC/DC Buck regulator was used to drive a Permanent Magnet DC (PMDC) motor [22]. This converter allows a unidirectional power flow that helps only DC motors' motoring operation. However, the abovementioned circuit cannot control the DC motor in the four quadrants, essential in DC drives. In [23], a four-quadrant DC chopper shown in Figure 4 was used to supply a separately excited DC motor's armature winding. This converter topology is preferred in DC drive applications to fulfill the four-quadrant operation, including motoring and reverse motoring.
However, this DC motor's field winding requires an additional DC source to energize the machine. The well-known applications of the different DC motor types and their power electronic converters are listed in Table I.

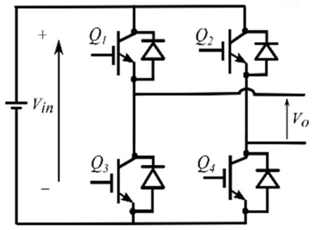

Figure 4. Class-E DC chopper

B. Stepper Motor Drives

Stepper motors (STMs) are prevalent in the heliostat drives units considering their relatively high torque at low speeds. Generally, STMs are classified into three main categories, i.e., variable reluctance STM, permanent magnet stepper motor (PM-STM), and hybrid stepper motor (HB-STM) [27]. A stepper motor's available features work at open-loop control and the high precision movement with non-accumulated movement error. Moreover, the absence of a commutator leads to less maintenance and a long lifetime. Therefore, no shaft encoder is needed to acquire the motor position [28]. Currently, STMs are used in the dual-axis tracking system for heliostat drives. Modeling and simulation of closed-loop control for STMs are presented in [29], where two sets of HB-STM drives are used to control an SPT located in Mexico. The power electronic circuit used to drive an STM depends on the number of stator phases, i.e., two, three, and four phases of stepper motors [30]. Therefore, the two-phase bipolar stepper motor requires two Class-E DC chopper modules were used in [29].

It is worth mentioning that the unipolar PM-STM, shown in Figure 5, is another configuration for PM-STMs, in which the phase mid-points are commonly connected to the ground to allow a unidirectional current flow in each half-coil. This configuration reduces the controlled switches used. However, it reduces the machine torque compared to the bipolar PM-STM working at the same step operation, i.e., full-, half-or micro-step control. Although this circuit is relatively cheaper and easier to control, it has not been used in the heliostat drive system yet to the best of the authors' knowledge. Hence, it is an exciting point to be investigated. A summary of power electronic converter circuits of the stepper motor is listed in Table I.

C. Induction Motors Drives

Induction motors (IMs) are widely employed in heliostat drive systems and industrial applications. They can produce relatively high torque at low speed, great accuracy, long lifetime, with the availability of several manufacturers in both small and large sizes. Besides, IMs have higher efficiency than DC motors for the same size and rating, mainly for increased ratings, making them very suitable for big-size solar tracking systems [17], [33], [34].

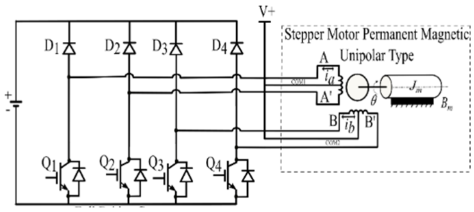

Figure 5. Power Circuit of unipolar PM Stepper Motor Model

Figure 6 shows the typical back-to-back converter used for three-phase IM drives. Variable frequency drive (VFD) and IMs are used together to provide smooth and accurate elevation and azimuthal movements. This method shows a feasible product [35]. A practical solution for double-axis solar tracking applications based on IMs was provided by Siemens [36]. Although the IM and VFD are preferred in industrial applications, this drive system's main drawback is implementing and justifying the control system compared to DC drives. Furthermore, for small rating heliostat units using PV as a supply, it is not easy to get a sufficient DC voltage to supply the IM VFD to drive the IM. Otherwise, an additional boost converter stage must be added, which is considered an extra cost. Moreover, Table I provides a rough guide of combinations of suitable motors and power electronic converters for a few typical applications.

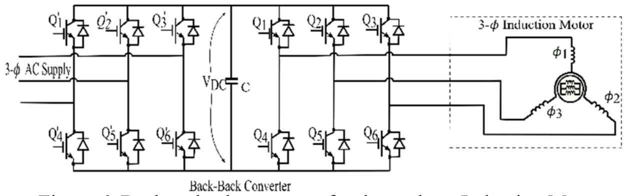

Figure 6. Back-to-back converter for three-phase Induction Motor

D. *Electrical Motor Drives Summary*

Based on the previous subsections' discussions, the different motors used in SPT systems, the IM is considered the superior motor according to the outstanding advantages. Additionally, the IM is regarded as the cheapest type according to the markets offering and the mass production [36], [42] - [43]. PM synchronous motors are rarely used in CSP applications as depicted in the different studies and the worldwide implemented plants. This point needs to be investigated to improve the PM synchronous performance and start to get SM drives' benefits in CSP applications. However, the PM motors have the drawback of relatively fast demagnetization of their magnets, particularly for such outdoor applications and at high ambient temperature levels, i.e., in Gulf Cooperation Council (GCC) countries [44]. Therefore, investigating the thermal stress on the PM-based motors is essential.

Regarding the power electronic converters, there are some common advantages and drawbacks for the different power electronic converter according to the essential components, i.e., thyristor, MOSFET, IGBT, and GTO. For instance, the MOSFET and IGBT-based converters, compared to the GTO and Thyristors ones, have faster response and lower losses, particularly at relatively high switching frequencies (several kHz to several hundreds of kHz). Besides, the most recent semiconductor technologies, i.e., the wide-band-gab (WBG) technologies, have lower turn-on and -off transitions. These semiconductor technologies reduce the converter switching losses and allow the converter's operation at high switching frequencies, impacting the electrical drives' performance [45]-[51]. Therefore, the WBG-based electrical drives utilized for SPT need more investigation.

5. Implemented SPT Prototype in KFUPM, KSA

An SPT prototype heliostat is designed and implemented in King Fahd University for Petroleum and Minerals (KFUPM), Dhahran, Kingdom of Saudi Arabia (KSA). A dual-axis drive system composed of two linear actuators was developed. A heliostat prototype of an adequate scale is employed to validate the theoretical study.

A block diagram for the dual-axis heliostat is shown in Figure 7. It consists of elevation and azimuth drives. Each drive system consists of a linear actuator based on a PMDC motor, and they are supplied from a class-E DC chopper. The model has been validated experimentally using a heliostat prototype. The experimental platform was tested for several days in different seasons to confirm the prototype capabilities for sun tracking during the whole year. Several days, experiments have been conducted to evaluate the drive system performance under several conditions. The integrated heliostat prototype is shown in Figure 8 - a. The location is the rooftop of an academic building at KFUPM in Dhahran, KSA. The drive system could reflect the sunbeams accurately, similar to the presented one-day results.

The drive system starts moving from the stow-position, as shown in Figure 8 – b, to the calculated heliostat angles for both azimuth and elevation angles. The tracking system could then follow the reference heliostat angles along the day. Figure 8. - c illustrates the heliostat operation instantly while the mirror reflects the sunbeams to the desired target. The experimental results of (Jul. 15th, 2020) from sunrise to sunset are presented in Figure 9 and Figure 10. These figures represent a comparison between the reference calculated angles and the measured angles. Therefore, the drive system starts moving from the stow-position to the calculated heliostat angles for both azimuth and elevation angles. The tracking system could then follow the reference heliostat angles along the day. By the end of the day, the heliostat drive is returned to the mirror to the stow-position at sunset at 6:30 P.M. The figure reflects that the drive system could follow the reference angles properly.

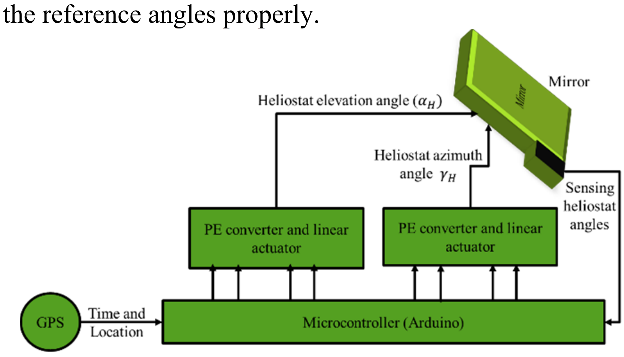

Figure 7. Block diagram of dual-axis solar tracking system

(a) (b) (c)

Figure 8. The proposed prototype of the automatic dual-axis solar tracking unit.

Table I: Typical motors, converter, and application guides

Type of Drive		Type of power electronic converters	Type of control	Applications
DC Drive [24]-[27]		• thyristor, AC/DC converter	• phase control with inner control loop	• automobiles for operating windshield wipers, • washers, blowers for air conditioners as well as heaters, • food mixers, electric toothbrushes, and moveable vacuum cleaners, • handy electric tools like hedge trimmers, drilling machines, etc. • traction applications, like locomotives, trolley cars, and starter motors in vehicles, • cranes and conveyor belt where higher starting torque is required
		• DC/DC converter (full H-bridge) GTO, IGBT, or MOSFET	• PWM control with internal control loop	• transportation, machine tools, and office equipment. • four quadrants DC drives
Stepper Drive [31], [32]		• DC/DC converter GTO, IGBT, or MOSFET	• phase current control with PWM	• 3D printing equipment, and printing presses, • automotive gauges and machine tooling automated Production equipment, • medical scanners, samplers, fluid pumps, respirators, and blood analysis machinery, • gaming machines, and small robotics, • CNC milling machines and welding equipment
Induction Drive [33] - [37]	Cage	• back-back thyristor	• phase control	• high torque, and low starting current, such as conveyors, compressors, crushers, agitators, reciprocating pumps
		• IGBT, GTO inverter, or Cycloconverter.	• PWM with *V-f* control	• standard torque and norm starting current, such as fans, blowers, centrifugal pumps, line shafting
		• IGBT, or GTO	• vector control	• high performance, such as sheers, punch presses, die stamping
	Slip ring	• thyristor AC/DC converter	• phase control with DC-link current control	• high torque, medium, and high slip, such as large pumps, fans, shears, punch presses, die stamping

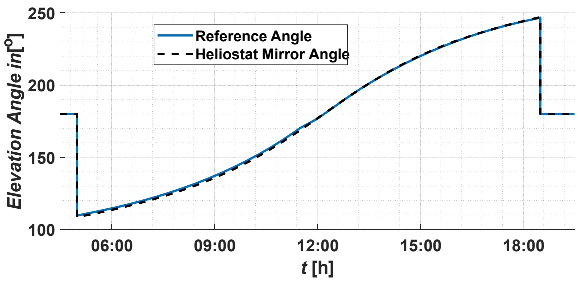

Figure 9: Reference and tracking angle for azimuth angle with heliostats mirror angles on Jun. 15th, 2020.

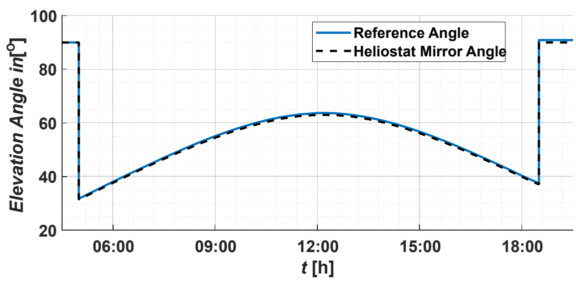

Figure 10. Reference and tracking angle for elevation angle with heliostats mirror angles on Jun. 15th, 2020.

6. Conclusion

This paper introduced a review of the different SPT drive systems, performance, and applications. The various electrical motors and their utilized power electronic converters used for SPT heliostat have been discussed. A summary of the electrical motors and the recent advancements of power electronic converters are discussed. The elevation-azimuth tracking model has been discussed in detail and developed for a dual-axis tracking system based on two linear-actuator drive systems. A complete DC-drive-based heliostat prototype is designed and implemented in KFUPM laboratories. As a good SPT technology location, the eastern province, KSA, is nominated to test the proposed prototype. The results showed the proposed drive system's accuracy and validated using the azimuth-elevation model for the dual-axis tracking system.

Acknowledgment

The authors gratefully acknowledge the support provided by King Fahd University of Petroleum & Minerals (KFUPM) (Grant No. GTEC1701), Saudi Arabia. Dr. Abido also acknowledges the support provided by K.A.CARE Energy Research & Innovation Center (ERIC), KFUPM.

References

[1] A. Pfahl, "Survey of Heliostat Concepts for Cost Reduction," *Journal of Solar Energy Engineering*, vol. 136, no. 1, 2014.
[2] U. Amita, and M. S. Soni. "Concentrating solar power–technology, potential and policy in India." *Renewable and Sustainable Energy Reviews*, vol. 15.9, pp. 5169-5175, 2011.
[3] M. T. Islam, N. Huda, A. B. Abdullah, and R. Saidur, "A comprehensive review of state-of-the-art concentrating solar power (CSP) technologies: Current status and research trends," *Renew. Sustain. Energy Rev.*, vol. 91, no. November 2017, pp. 987–1018.
[4] Q. Xie, Y. Xiao, X. Wang, D. Liu, and Z. Shen, "Heliostat cluster control for the solar tower power plant based on leader-follower strategy," *IEEE Access*, vol. 7, pp. 135031–135039, 2019.
[5] Y. Hu, Z. Xu, C. Zhou, J. Du, and Y. Yao, "Design and performance analysis of a multi-reflection heliostat field in solar power tower system," *Renew. Energy*, vol. 160, pp. 498–512, 2020.
[6] Y. Xiao, Q. Xie, and Z. Deng, "A Review on Heliostat Field Layout and Control Strategy of Solar Tower Thermal Power Plants," *Proc. 2018 Chinese Autom. Congr. CAC 2018*, pp. 1909–1912, 2019.
[7] T. Pavlović, I. Radonjić, D. Milosavljević, and L. Pantić, "A review of concentrating solar power plants in the world and their potential use in

Serbia*." Renewable and Sustainable Energy Reviews, vol.* 16.6, pp. 3891-3902, 2012.

[8] S. Rech, A. Lazzaretto, and E. Grigolon, "Optimum integration of concentrating solar technologies in a real coal-fired power plant for fuel-saving*," Energy Convers. Manag.,* vol. 178, no. September 2018, pp. 299–310.

[9] G. Manente, S. Rech, and A. Lazzaretto, "Optimum choice and placement of concentrating solar power technologies in integrated solar combined cycle systems," *Renew. Energy*, vol. 96, pp. 172–189, 2016.

[10] A. Ummadisingu and M. Soni, "Concentrating solar power – Technology, potential, and policy in India," *Renewable and Sustainable Energy Reviews*, vol. 15, no. 9, pp. 5169-5175, 2011.

[11] H. Zhang, J. Baeyens, J. Degrève, and G. Cacères, "Concentrated solar power plants: Review and design methodology," *Renewable and Sustainable Energy Reviews*, vol. 22, pp. 466-481, 2013.

[12] R. I. Dunn, P. J. Hearps, and M. N. Wright, "Molten-Salt Power Towers: Newly Commercial Concentrating Solar Storage," Proceedings of the IEEE, vol. 100, no. 2, pp. 504–515, 2012.

[13] "IRENA solar atlas." [Online]. Available: https://solarpaces.nrel.gov-/by-country.

[14] A. Peinado Gonzalo, A. Pliego Marugán, and F. P. García Márquez, "A review of the application performances of concentrated solar power systems," *Appl. Energy*, vol. 255, no. July, p. 113893, 2019.

[15] J. N. Larmuth, "Heliostat cost reduction methods applied to a small heliostat," *2015 Univ. Stellenbosch, MS,* no. December 2015.

[16] U. Jakobsen, K. Lu, P. O. Rasmussen, D.-H. Lee, and J.-W. Ahn, "Sensorless Control of Low-Cost Single-Phase Hybrid Switched Reluctance Motor Drive," *IEEE Transactions on Industry Applications*, vol. 51, no. 3, pp. 2381–2387, 2015.

[17] A. Pfahl, M. Randt, C. Holze and S. Unterschütz, "Autonomous light-weight heliostat with rim drives", *Solar Energy*, vol. 92, pp. 230-240, 2013.

[18] W. M. Hamanah, A. Salem, M. A. Abido, A. M. Qwbaiban, and T. G. Habetler, "Solar Power Tower Drives: A Comprehensive Survey," in IEEE Access, doi: 10.1109/ACCESS.2021.3066799.

[19] Arshad H., et al. (2019). Weighting factors optimization of model predictive torque control of induction motor using NSGA-II with TOPSIS decision-making. *IEEE Access*, *7*, 177595-177606.

[20] H. Satpathi, G. K. Dubey and L. P. Singh, "A General Method of Analysis of Chopper Fed DC Separately Excited Motor," in *IEEE Transactions on Power Apparatus and Systems*, vol. PAS-102, no. 4, pp. 990-997, April 1983.

[21] M. R. Erickson and J. A. Kaehler, "*Heliostat control employing direct current motor*," Aug. 20th, 1985, US Patent 4,536,847.

[22] L. Zi-Yi, W. Sew-Kin, P. Wai-Leong, and O. Chee-Pun, "The design of dc motor driver for solar tracking applications," *Proc. IEEE Int. Conf. Semicond. Electron. (ICSE),* Sep. 2012, pp. 556–559.

[23] A. Zeghoudi and A. Chermitti, "Speed Control of a DC Motor for the Orientation of a Heliostat in a Solar Tower Power Plant using Artificial Intelligence Systems (FLC and NC)," *Research Journal of Applied Sciences, Engineering and Technology*, vol. 10, no. 5, pp. 570-580, 2015.

[24] IEEE Standard Practices and Requirements for Thyristor Converters for Motor Drives Part 1- Converters for DC Motor Armature Supplies," in *ANSI/IEEE Std 444-1973*, vol., no., pp.1-98, Jan. 25th, 1974.

[25] M. Muruganandam and M. Madheswaran, "Performance analysis of fuzzy logic controller-based DC-DC converter fed DC series motor," *2009 Chinese Control and Decision Conference*, Guilin, 2009, pp. 1635-1640.

[26] A. Pashaei, M. T. Haque and S. Alizadeh, "Control of Output Voltage of Simple DC-DC Converters," *2006 IEEE Vehicle Power and Propulsion Conference*, Windsor, 2006, pp. 1-5.

[27] D. S. C. W., *Sensors and actuators: Engineering System Instrumentation*. Boca Raton, FL: CRC Press, 2016.

[28] N. Greenough and C. C. Kung, "A new high-efficiency stepper motor driver for old technology stepper motors," *2013 IEEE 25th Symposium on Fusion Engineering (SOFE)*, 2013.

[29] D. S. Ramteke and M. B. Gaikwad, "Isolated DC-DC Converter Fed DC Motor for Bidirectional Electric Vehicular Application," *2018 International Conference on Smart Electric Drives and Power System (ICSEDPS)*, Nagpur, 2018, pp. 33-37.

[30] H. Moczala, J. Draeger, H. Krauss, H. Schock, and S. Tillner, "Small Electric Motors, Stepper motors -principles and applications," *Stevenage: IET* (308 p.). 1998.

[31] IEEE Standard Practices and Requirements for Thyristor Converters for Motor Drives Part 1- Converters for DC Motor Armature Supplies," in *ANSI/IEEE Std 444-1973*, vol., no., pp.1-98, Jan. 25th, 1974.

[32] M. Muruganandam and M. Madheswaran, "Performance analysis of fuzzy logic controller-based DC-DC converter fed DC series motor," *2009 Chinese Control and Decision Conference*, Guilin, 2009, pp. 1635-1640.

[33] B. Aichi, M. Bourahla, and K. Kendouci, "Real-time nonlinear speed control of an induction motor based on a new advanced integral backstepping approach," *Trans. Inst. Meas. Control*, vol. 42, no. 2, pp. 244–258, 2020.

[34] R. Gunabalan, P. Sanjeevikumar, F. Blaabjerg, O. Ojo and V. Subbiah, "Analysis and Implementation of Parallel Connected Two-Induction Motor Single-Inverter Drive-by Direct Vector Control for Industrial Application," *IEEE Transactions on Power Electronics*, vol. 30, no. 12, pp. 6472-6475, Dec. 2015.

[35] J. Enrile, P. Valera, and R. Osuna, "Prothelios: heliostat for large PV plants," *3rd World Conference Photovolt. Energy Convers.*, pp. 2386–2388, 2003.

[36] Siemens, "How to exploit sunlight toward maximum energy yield?" [Online]. Available: https://eandm.com/media/EandM/PDFs/ Siemens Solar.pdf, Accessed: Feb. 2020.

[37] S. Zhang, A. M. Qwbaiban and T. G. Habetler, "A Survey of Electric Drives for Solar Tracking Control of Concentrated Solar Power Heliostats," *IECON 2019 - 45th Annual Conference of the IEEE Industrial Electronics Society, Lisbon, Portugal*, 2019, pp. 2288-2294.

[38] A. K. Wallace, M. S. Boger and E. Wiedenbrug, "Medium- and high-voltage, low-speed drives using low-voltage IGBT converters," *1995 Proceedings of the IEEE International Symposium on Industrial Electronics*, Dubrovnik, 1995, pp. 86-90 vol.1.

[39] A. A. Radionov, O. S. Malakhov, S. N. Baskov, A. S. Konkov, and M. S. Davydkin, "The design features of the converters for synchronous motors vector-pulsed launch control," *2010 IEEE Region 8 International Conference on Computational Technologies in Electrical and Electronics Engineering (SIBIRCON)*, Listvyanka, 2010, pp. 608-610.

[40] L. Rovere, A. Formentini, G. L. Calzo, P. Zanchetta, and T. Cox, "IGBT-SiC dual fed open-end winding PMSM drive," *2017 IEEE International Electric Machines and Drives Conference (IEMDC)*, Miami, FL, 2017, pp. 1-7.

[41] M. F. Rahman, P. Niknejad and M. R. Barzegaran, "Comparing the performance of Si IGBT and SiC MOSFET switches in modular multilevel converters for medium voltage PMSM speed control," *2018 IEEE Texas Power and Energy Conference (TPEC)*, College Station, TX, 2018, pp. 1-6.

[42] F. Sloan, S. Bull, and R. Longerich, "Design Modifications to Increase Fatigue Life of Fiber Ropes," in Proc. of the 2005 IEEE/MTS OCEANS Conference (OCEANS 2005), Washington, DC, September 2005, pp. 829–835.

[43] K. Ueura and R. Slatter, "ACTUATORS: Development of the harmonic drive gear for space applications," in Proc. of the 8th European Symposium on Space Mechanisms and Tribology), Toulouse, Fr, October 1999, pp. 829–835.

[44] D. Kim, D. H. Kang, C. Kim, J. Kim, Y. Kim, and S. Jung, "Operation Characteristic of IPMSM Considering PM Saturation Temperature," in *IEEE Transactions on Applied Superconductivity*, vol. 30, no. 4, pp. 1-4, June 2020, Art no. 5207204, DOI: 10.1109/TASC.2020.2989799.

[45] A. Salem, "Design, Implementation, and Control of a SiC-Based T5MLC Induction Drive System," in *IEEE Access*, vol. 8, pp. 82769-82780, 2020, DOI: 10.1109/ACCESS.2020.2991691.

[46] W. M. Hamanah, A. Salem, and M. A. Abido, "Heliostat Dual-Axis Sun Tracking System: A Case Study in KSA," *18th International Conference on Renewable Energies and Power Quality (ICREPQ'20) Granada (Spain), 1st to Apr. 2nd, 2020.*

[47] A. Salem and M. A. Abido. "T-type multilevel converter topologies: A comprehensive review." *Arabian Journal for Science and Engineering* 44, no. 3 (2019): 1713-1735.

[48] M. Fernández *et al*., "Short-Circuit Study in Medium-Voltage GaN Cascades, p-GaN HEMTs, and GaN MISHEMTs," *IEEE Transactions on Industrial Electronics*, vol. 64, no. 11, pp. 9012-9022, Nov. 2017, DOI: 10.1109/TIE.2017.2719599.

[49] C. A. Belhadj, W. M. Hamanah and M. Kassas, "LabVIEW based real time Monitoring of HVAC System for Residential Load," *2017 IEEE International Conference on Computational Intelligence and Virtual Environments for Measurement Systems and Applications (CIVEMSA)*, Annecy, France, 2017, pp. 66-71, doi: 10.1109/CIVEMSA.2017.7995303.

[50] X. Zhang, G. Qin and C. Fan, "The Contact Type of Ag-Gan Piezoelectric Semiconductor via Experiment," *2019 13th Symposium on Piezoelectricity, Acoustic Waves and Device Applications (SPAWDA)*, Harbin, China, 2019, pp. 1-4.

[51] A. Salem, et al., "Capacitor Balancing and Common-Mode Voltage Reduction of a SiC Based Dual T-Type Drive System Using Model Predictive Control," in *IEEE Access*, vol. 7, pp. 41066-41077, 2019.